

Measurement of Effective Stress Intensity Factor Range of Mode II Fatigue Crack Growth using Hysteresis Loop

Shigeru Hamada^{1,*}, Minjian Liu²

¹ Department of Mechanical Engineering, Faculty of Engineering, Kyushu University,
744 Moto-oka, Nishi-Ku, Fukuoka 819-0395, Japan

² Department of Mechanical Engineering, Graduate School of Engineering, Kyushu University,
744 Moto-oka, Nishi-Ku, Fukuoka 819-0395, Japan

* Corresponding author: hamada@mech.kyushu-u.ac.jp

Abstract A method was proposed for measuring the effective stress intensity factor ranges of Mode II fatigue crack growth by using the hysteresis loop for a specimen's surface strain. Many cases of rolling contact fatigue failure, such as those that occur in railway rails, bearings and gears are due to repeated high shear loads. In order to prevent such fatigue failures, the resistance of a material to repeated high shear loads must be determined. The fatigue crack growth characteristics are dependent on the Mode II stress intensity factor range. However, conventionally measured Mode II fatigue crack growth characteristics vary according to the measurement methods. Therefore, the authors improved the experimental measurement method proposed by Murakami, and proposed a way to measure the Mode II effective stress intensity factor range. Improvements to the jigs and specimen were made based on the ideal mechanical model of the experimental method. Furthermore, to measure the Mode II fatigue crack growth behavior, strain gauges were applied to the specimen and the hysteresis loop of the strain was measured with high accuracy by using a newly developed subtraction circuit.

Keywords Rolling contact fatigue, Friction, Mode II fatigue crack, Effective stress intensity factor, Fracture mechanics

1. Introduction

Mechanical failures such as spalling and pitting can occur in rails, bearings, and other components when they are subjected to heavy repeated rolling contact loading. In order to prevent these types of failures, it is necessary to determine the resistance of certain materials to them. A fatigue crack under repeated rolling contact loading, which is what leads to the failure, propagates in Mode II. Therefore, the resistance to fatigue crack propagation which is caused by stress concentration sources such as flaws or inclusions can be evaluated by using the Mode II fatigue threshold stress intensity factor range, ΔK_{IIth} .

Methods for measuring Mode I fatigue crack propagation have already been established and standardized [1]. However, for Mode II fatigue crack propagation, systematic research is limited because this type of fatigue crack propagation is difficult to produce in a laboratory and there are no standard tests. Early systematic research was conducted by Otsuka et al. [2]. However, the method they developed could only be applied to soft metals such as aluminum alloys, even though hard metals are used for the components for which Mode II fatigue crack become a problem. After this study, Murakami et al. [3, 4] developed an experimental method that could also be applied to hard metals such as bearing steel. Later, Otsuka et al. [5] improved their method so that it could also be applied to hard metals. However, different values were obtained for the threshold stress intensity factor range ΔK_{IIth} when these two methods [4, 5] were used for the same material. It seems that interference by the crack faces affected the result. The study conducted by Matsunaga et al. [6] on the shear mode threshold proved that friction on the crack face increases the value of ΔK_{IIth} . Therefore, it is thought to be necessary to take the friction on the crack faces into account when determining the Mode II effective stress intensity factor range, ΔK_{IIeff} .

In the previous work by the authors, a new method was proposed [7, 8] to measure the friction at the crack faces and ΔK_{IIeff} . Moreover, a more appropriate assumption for the friction distribution on

the crack faces was made and a new method was proposed. This paper discusses, Mode II fatigue crack growth experiments that were conducted using the proposed method, along with the obtained results.

2. Experimental procedures

2.1. Mechanical model

Figure 1(a) shows the mechanical model of the Mode II fatigue crack growth experiment that was proposed by Murakami et al. [3]. In this paper, this model is referred to as the “former mechanical model.” Load P was applied to the upper cantilever. By inserting a ceramic cylinder in the slit, load P was assumed to be divided into two equal halves and applied to both cantilevers. In a real machine, a Mode II crack propagates under the condition of compressive stress. Therefore compressive load S was applied using the pre-tightening force of bolts. Mode II fatigue crack growth experiments were performed by applying the former mechanical model. However, because of the plastic deformation of the specimen where the ceramic cylinder made contact with it, load P could not be divided as expected. In fact, dents were found on the specimen where the ceramic cylinder inserted into the slit made contact, and a considerable reduction in the slit width was observed during the fatigue experiment. This reduction in the slit width was thought to be caused by a gap formed as a result of plastic deformation when the load was applied and, as a result, the load applied to the lower cantilever was thought to be considerably reduced.

In order to equally divide the load P between the cantilevers, a new mechanical model has been proposed [7, 8]. Figure 1(b) shows this new mechanical model, which was based on the experimental setup shown in Fig. 1(c). The new model was discussed with springs and rigid blocks in the previous study [7, 8]. This discussion showed that if the pre-tightening force S was larger than $P/2$, then the load was divided into two equal halves and applied to the two cantilevers, and the width of the slit did not change during the experiment even if a cylinder was not in place. In addition to the compressive load S by the pre-tightening force of the bolts, compressive load Q was applied on the fatigue crack face in order to avoid crack branching in Mode I during the fatigue crack propagation.

2.2. Material

The experiments were carried out using commercial grade Japanese Industrial Standards (JIS) SS400 steel (400 MPa minimum tensile strength) which is rolled steel designed for general structures. Table 1 presents its chemical composition.

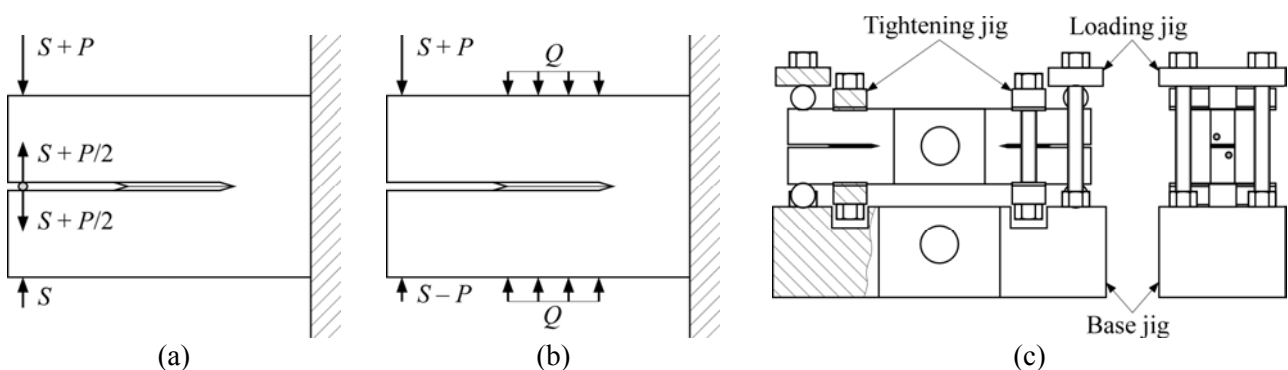


Figure 1. Mechanical models for Mode II experimental method: (a) former mechanical model [3], (b) new mechanical model [7, 8], and (c) new experimental setup

2.3. Specimen

Figure 2 shows the shape and dimensions of the specimen that was used in this study. The specimen had a chevron notch and side grooves. The fatigue crack initiated at the tip of the chevron notch, where the stress intensity factor was high. The groove on the side of the chevron notch caused Mode II fatigue crack growth in the section with the maximum shear stress and prevented crack branching in the direction of the maximum tensile stress, which was a Mode I crack. Two crack propagations were simultaneously carried out on a single specimen. Compressive force Q was applied on the crack face with the middle jigs to avoid crack branching in Mode I. In order to reduce the unexpected horizontal force applied to the specimen, three of the four grooves on the end of the cantilever were made flat and one was made larger with a radius of 1 mm to 4 mm. The three flat grooves allowed for the relative displacement caused by the elastic deformation between the specimen and the jigs. The large circular groove prevented the specimen from moving.

2.4. Experimental setup

Figure 3 shows the setup of the experiment. Four ceramic cylinders were placed between the cantilevers and the loading jigs. As a result, the load applied to the specimen was divided into two equal halves on the cantilevers. A cyclic tensile load P in the form of a sine wave, ranging from 0.5 kN to 10 kN (stress ratio: $R = 0.05$) was applied to the center holes in the jig and specimen through two pins using a servo-hydraulic fatigue testing machine operating at a frequency of 6 Hz. In order

Table 1. Chemical composition of specimen (mass %)

C	Si	Mn	P	S	Fe
0.11	0.27	0.55	0.021	0.023	Bal.

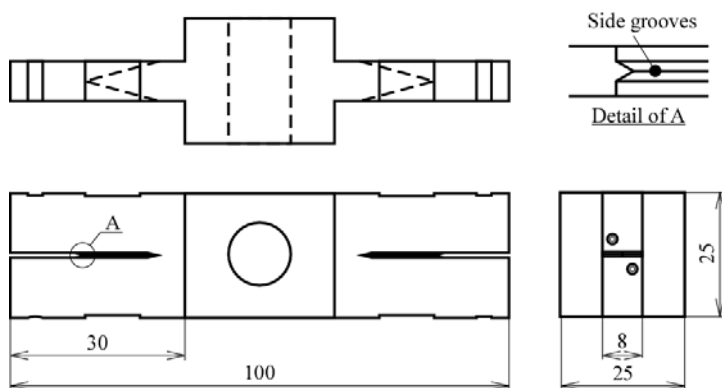


Figure 2. Shape and dimensions of specimen (unit: mm)

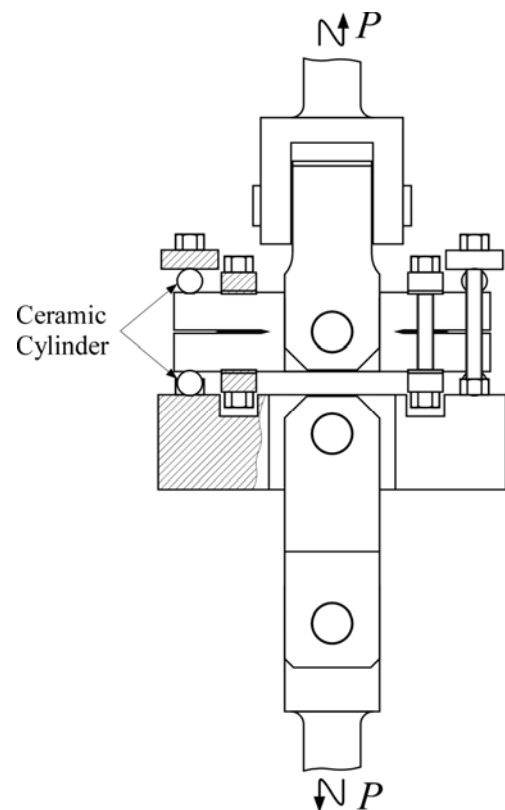


Figure 3. Experimental setup

to suppress the tendency for Mode I crack branching, the pre-tightening load S of a bolt was applied to the ends of the cantilevers and vertical compressive load Q was applied to the crack faces using the loading jigs and tightening jigs. The ceramic cylinder diameter (8 mm) was larger than that used in the former setup (1 mm) in order to reduce the plastic deformation of the specimen on the contact face. Moreover, a set of universal joints was used to cancel out the unexpected moment applied to the specimen.

The specimen and jigs were designed considering their compatibility with the fatigue crack growth experiment equipment using a “CT (Compact Tension) specimen.” Therefore, the experimental setup shown in Fig. 3 could be used with environmental experiments equipment that is designed for a “CT specimen.”

2.5. Crack length measuring method

The crack length during the fatigue crack growth experiment was measured by using the AC potential method [3]. Two electrodes were connected to the ends of the cantilevers. As the crack between the two cantilevers grew, the electrical resistance between these two electrode points increased. Then, the resistance was measured and converted into the crack length. The ratio of the increase in the electric potential (ΔE) caused by the crack growth to the electric potential at the beginning of the experiment (E_0) correlated with the crack length. Therefore, the crack length could be measured without interrupting the experiment. The specimen was insulated from the jig using the ceramic cylinders.

3. Derivation of friction between crack faces

In order to measure the friction between the fatigue crack faces, two strain gauges (Kyowa Electronic Instruments Co., Ltd., KFG-2N-120-C1) were placed on the specimen surface. Figure 4 shows the strain measurement positions on the specimen. The friction force on the crack face was derived from the load-strain curve over one cycle using the outputs of the strain gauges.

Figure 5 shows the basic model for the derivation of the friction, which represents a mass spring model with a rough ground and a mass subjected to a cyclic load P . The load-displacement curve over a cycle is shown in Fig. 5(b). Because the direction of the friction changes over a cycle, the friction can be derived from the hysteresis in the load-displacement curve.

However, for the real experiment, the curve became more complicated. When the loading began, the portion of the crack faces at the notch began to slide, and all of the other parts of the crack faces soon followed. As a result, the linear part of the curve marked (i) became nonlinear. Thus, because of the plastic deformation that occurred around the crack tip, the portion of the linear part of the curve marked (ii) also became nonlinear. The same phenomena also occurred at the portions marked (iii) and (iv). Therefore, the load-strain curve over one cycle was estimated to be that is shown in Fig. 6. The friction could still be derived from the load-strain curve. The vertical dashed line shown in Fig. 6 starts from point A and intersects at point B with the extended line of the elastic portion of the curve at the unloading. The length of dashed line AB is related to the friction, where the relation is determined using a finite element method (FEM).

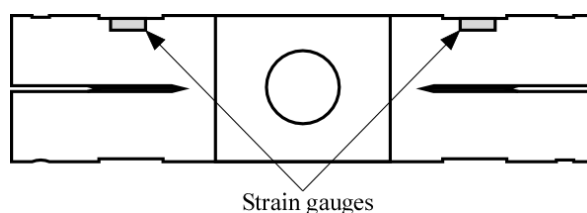


Figure 4. Strain gauges placed on specimen

4. Results and discussion

The fatigue crack growth experiment was ended by the action of the displacement limiter at $N = 2.08 \times 10^6$ cycles. A fatigue crack that nucleated and grew at the root of the cantilever caused the limiter action. Figure 7 shows the displacement range ($\Delta\delta$) of the load piston during the fatigue experiment. Until $N = 1.0 \times 10^6$ cycles, the displacement range maintained a constant value. However, at $N = 2.0 \times 10^6$ cycles, the value rose slightly and then suddenly began to increase. This sudden increase was thought to indicate the fatigue crack growth at the root of the cantilever. Therefore, in this case, the intended fatigue crack growth experiment was performed until around $N = 1.0 \times 10^6$ cycles.

4.1. Mode II fatigue crack growth behavior

Figure 8 shows the relationship between the potential difference and the number of cycles measured using the AC potential method. In this experiment, because the effect of electric noise was not removed, averaged data were considered. From Fig. 8, it can be seen that the crack began to grow from $N = 5 \times 10^3$ cycles, after which the crack growth depended on the number of cycles.

4.2. Fracture surface of Mode II fatigue crack

After the fatigue crack growth experiment, the fracture surface was observed using a scanning electron microscope (SEM). Figure 9 shows the result of this observation. In this figure, lines that were parallel to the crack growth direction and cracks branching in the Mode I direction were found, which are characteristic of a Mode II fatigue fracture surface [3, 4]. Therefore, the success of the Mode II fatigue crack growth experiment was verified.

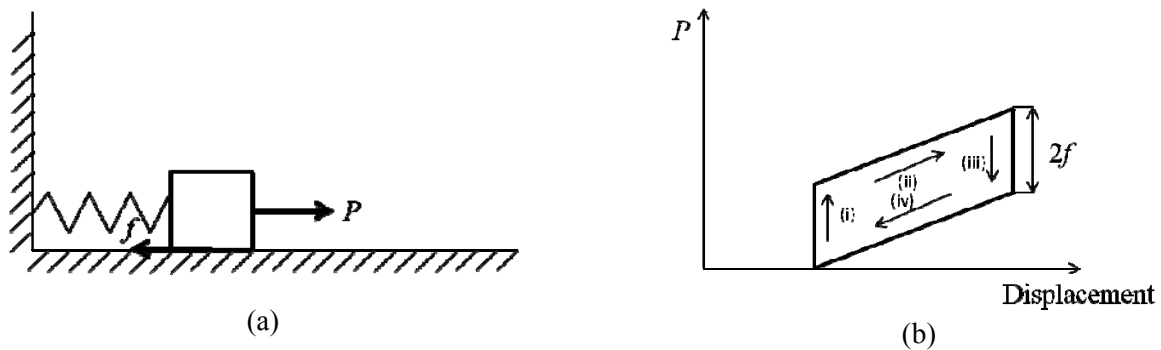


Figure 5. Models for derivation of friction: (a) mass-spring model and (b) load-displacement curve

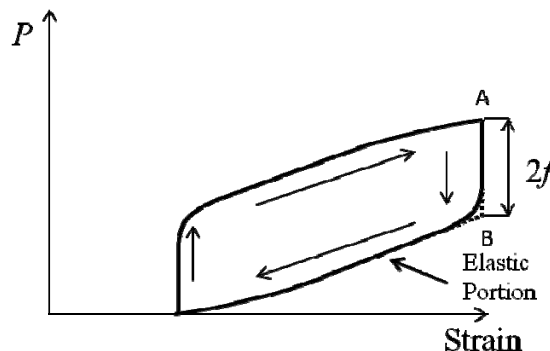


Figure 6. Estimated load-strain curve

4.3. Friction force measurement

Figure 10(a) shows an example of the relationship between the load and the strain at $N = 4.0 \times 10^4$ cycles. In order to measure the hysteresis loop of the strain with high accuracy, a subtraction circuit was developed. The input data were the strain at a jig and the strain at a specimen, as measured by strain gauges. These strains were converted to electric potentials and subtracted in the circuit. Figure 10(b) shows that the relationship between the load and the subtracted strain. From Fig. 10(b), the hysteresis loop was observed during a load cycle. As seen from a comparison of Fig. 10(b) with Fig. 6, the hysteresis loop was the same at a low load, whereas a difference existed at a high load. At present, the exact reason for this result is not known. However, through an analysis of the obtained load-strain hysteresis loop, the friction force and values of $\Delta K_{II\text{eff}}$ and $\Delta K_{II\text{th}}$ could be determined in a future study.

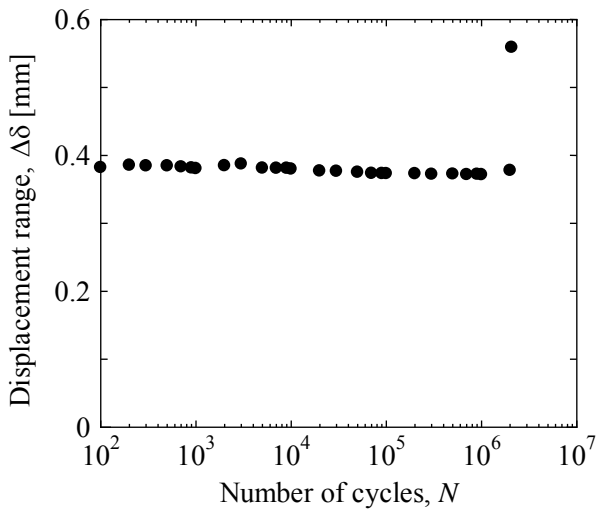


Figure 7. Relationship between displacement range of pull-rod and number of cycles

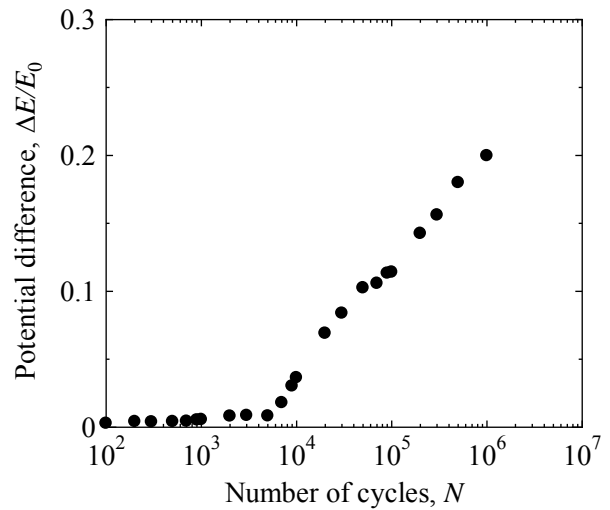


Figure 8. Relationship between potential difference and number of cycles

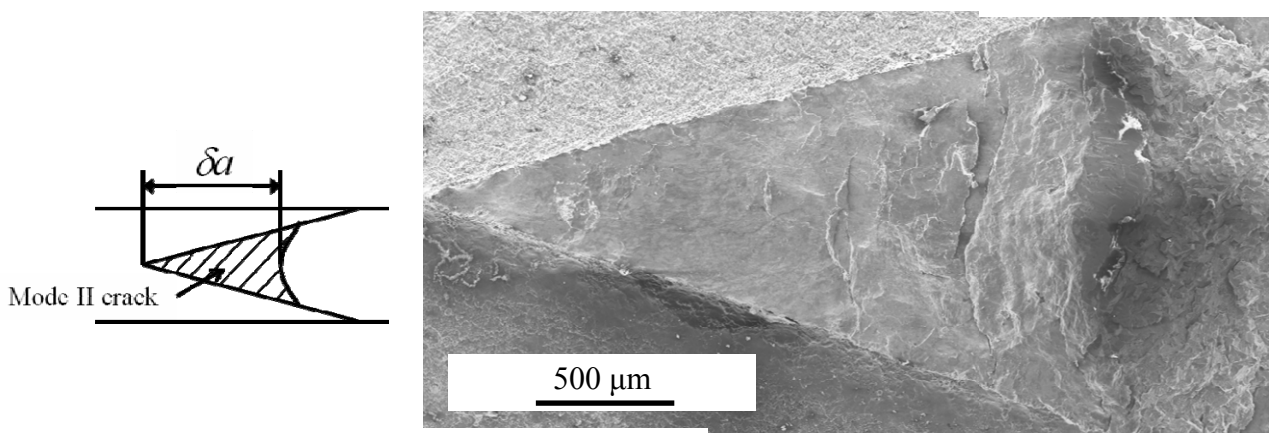


Figure 9. Fracture surface of Mode II fatigue crack

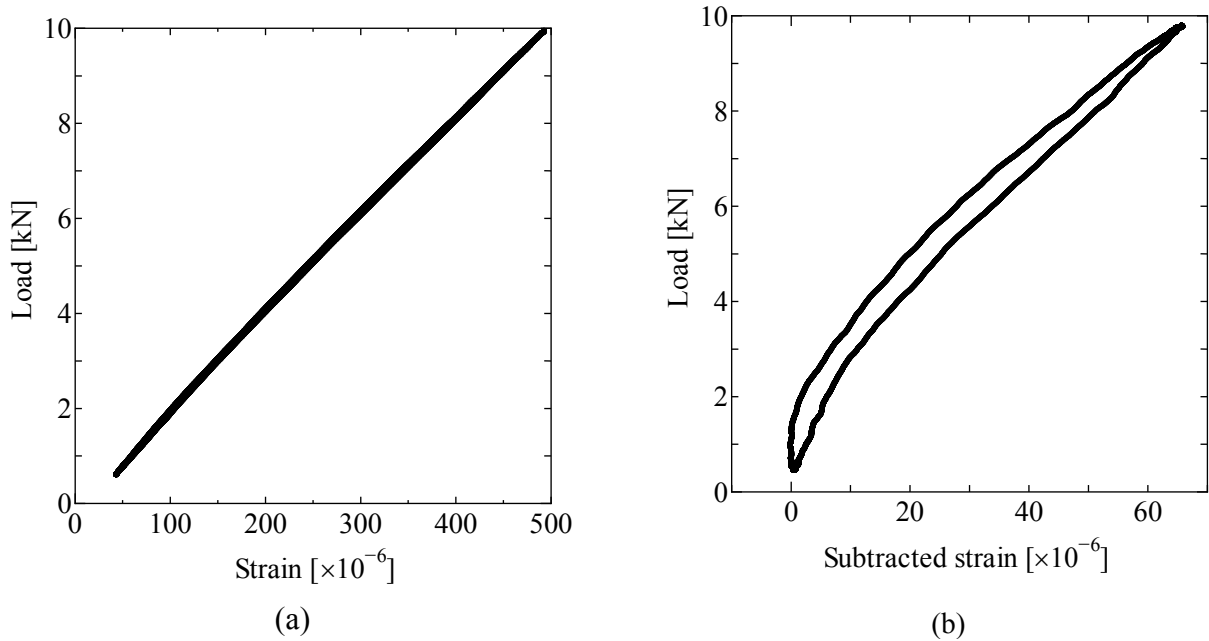


Figure 10. Example of relationship between load and strain (at $N = 4.0 \times 10^4$ cycles): (a) strain is measured strain and (b) strain is subtracted strain

5. Conclusions

The mechanical model for the Mode II experimental method proposed in the previous paper was modified. Thus, the load was considered to be equally divided into two halves and applied to each cantilever of the specimen. Furthermore, a new method for determining the friction between the crack faces was proposed. The crack length and friction between the crack faces were measured using an AC potential method and deduced from the load-strain curve, respectively. From this measurement and deduction, $\Delta K_{II\text{eff}}$ could be determined. However, the value of $\Delta K_{II\text{th}}$ has not yet been determined. It will be determined using this method in a future study.

Acknowledgements

This work was supported by JSPS KAKENHI Grant Number 24560103.

References

- [1] American Society for Testing and Materials, ASTM E647-11^{e1}: Standard test method for measurement of fatigue crack growth rates, 2011.
- [2] A. Otsuka, K. Mori and K. Tohgo, Current research on fatigue cracks, material research series, The society of materials science, Japan, 1 (1985) 127-55.
- [3] Y. Murakami, S. Hamada, Fatigue Fract. Engng. Mater. Struct., 20 (1997) 863-70.
- [4] Y. Murakami, C. Sakae and S. Hamada, Engineering Against Fatigue, edited by J. H. Beynon, M.W. Brown, T. C. Lindley, R. A. Smith & B. Tomkins, Taylor & Francis, UK.
- [5] A. Otsuka, Y. Fujii and K. Maeda, Fatigue Fract. Engng. Mater. Struct., 27 (2004) 203-212.
- [6] H. Matsunaga, N. Shomura, S. Muramoto and M. Endo, Fatigue Fract. Engng. Mater. Struct., 34 (2011) 72-82.
- [7] M. Liu, S. Hamada, Procedia Engineering, 10 (2011) 1949-1954.
- [8] M. Liu, S. Hamada, Proceedings of 19th European Conference on Fracture (ECF19), (2012) ID 455.

